

PAPER • OPEN ACCESS

## CubeSat satellite patch antenna designed with 3D printable materials: a numerical analysis

To cite this article: Erika Pittella *et al* 2023 *J. Phys.: Conf. Ser.* **2526** 012042

View the [article online](#) for updates and enhancements.

You may also like

- [Water and xenon ECR ion thruster—comparison in global model and experiment](#)  
Yuichi Nakagawa, Hiroyuki Koizumi, Yuki Naito et al.
- [Thermal Validation Testing of an Automatic Identification System \(AIS\) Receiver for Low Earth Orbit \(LEO\) CubeSat](#)  
Emir Husni and Nazmi Febrian
- [Static and Random Vibration Analyses of a University CubeSat Project](#)  
George I. Barsoum, Hesham H. Ibrahim and Mina A. Fawzy

# CubeSat satellite patch antenna designed with 3D printable materials: a numerical analysis

Erika Pittella, Livio D'Alvia and Emanuele Piuzzi

erika.pittella@unipegaso.it, livio.dalvia@uniroma1.it, emanuele.piuzzi@uniroma1.it

corresponding author: erika.pittella@unipegaso.it

**Abstract.** The paper presents a compact patch antenna system designed using 3D printable materials and compatible with any CubeSat satellite structure. Small satellites are transforming the space industry, allowing space access with an important cost reduction for satellite industries and a shorter plan development time compared to bulky satellites. Moreover, using additive manufacturing, it is possible to design specific system components, also with a complex geometry of the inner part, without material wasting. Furthermore, a key point of 3D printing is to allow to go from design to construction straight, having an enormous effect on the supply chain. Generally, CubeSats count on Very High Frequency and Ultra High Frequency communication systems for low bit-rate uplink and downlink. Instead, S-band is among the favourite choices for high bit rates since the frequency range 2.40–2.45 GHz is one of the International Telecommunication Union (ITU) amateur satellite frequency range. An S-band printed antenna system is designed in the present paper, considering the limitations on size and the weight of CubeSat standard. The antenna system is simulated with an electromagnetic CAD, using the polylactic acid as substrate, or polylactide, a thermoplastic polyester widely used in 3D printing.

## 1. Introduction

Small satellites equipped with advanced electronics and sensor systems, weighing from 1 to 50 kg, can be applied in a large range of satellite applications, for example technology validation, Earth observation, space exploration, with a low mission cost [1, 2]. According to the literature [2], there are currently around 3000 artificial satellites in orbit, about 2000 of which are in low-Earth orbit, i.e., up to altitudes of 2000 km and it is very probable that this number will increase by orders of magnitude in the next decade [3]. This growth represents a great opportunity but, at the same time, increases the debris problem, a topic already faced by several research groups [4]-[6].

Depending on the specific mission, a satellite has to satisfy some requirements and it also has to fulfill CubeSat standards that limit dimensions and weight: in this way, the subsystem design is challenging.

The communication subsystem is a very relevant component of a satellite since it ensures the uplink of telecommands and the downlink of telemetry. Specifically, the antenna design has to consider both mission aspects and CubeSat size-constraints [7]. Typically, S-band is the favorite choice for high bit-rates since this band is within the ITU International amateur satellite frequency band [8]. For these reasons, one of the most important features of satellite missions is the antenna design. Furthermore, depending on the particular mission, the design of specific antenna radiation patterns appears to be crucial [9].



Moreover, access to space for research missions and educational purposes requires that the cost of the components should be as low as possible and the production time short. Furthermore, the possibility to build a complex geometry in an effortless way suggests the design of the antenna with 3D printing. Indeed, using additive manufacturing, it is possible to build customized system components, with complex geometry, without wasting of material. A key point of 3D printing is to go from production to consumption straight, having an enormous effect on the supply chain. The polylactic acid, or polylactide (PLA) is the most commonly used plastic filament material in 3D printing. It is a widespread material produced from renewable resources, since it is naturally made from fermented vegetable starch as for example sugarcane, corn, cassava or sugar beet pulp [10]. The derivation of the PLA from renewable sources makes it biodegradable; moreover, another important key point is the recycling option [10].

The present paper shows the design of a patch antenna, carried out with Microwave Studio (MWS) by Computer Simulation Technology (CST), a full EM CAD based on the FIT method and the design of the feeding microstrip input line achieved with the CAD Microwave Office (MWO<sup>TM</sup> Applied Wave Research). The whole design has been optimized using as substrate a material having the characteristics of PLA filament Filoalfa<sup>®</sup> [11].

The reminder of the paper is organized as follows: in Section 2 methods and models are presented, results of the antenna parameters are shown in Section 3, and finally, in Section 4 conclusions are described.

## 2. Methods and Models

### 2.1. Substrate material

The substrate considered for the patch antenna design is the PLA, whose properties ( $\epsilon=2.1$ ,  $\tan\delta=0.005$ ) have been characterized in [12]. In particular, a similar behavior with respect to polytetrafluoroethylene (PTFE), a synthetic fluoropolymer of tetrafluoroethylene with numerous applications, was found. It is worth noting that PTFE has outstanding dielectric properties, particularly at high radio frequencies, it is appropriate for use as insulator in connector and cables, and in PCBs used at MW frequencies [13].

In order to achieve a dependable system, a multi-layer design has been chosen with a layer's configuration as shown in Fig. 1. In particular, the patches are fabricated on a 1.52 mm-thick PLA substrate hosting a ground plane on the opposite face; the antenna phasing and feeding network is fabricated on a thinner PLA substrate (0.508 mm) having the same ground plane of the antenna. This is convenient, because the face where the antenna is mounted (bottom face of the CubeSat) generally needs some free space, i.e., for the solar panels or a camera, in case of observation missions; therefore, some space at the center of the face has been left.

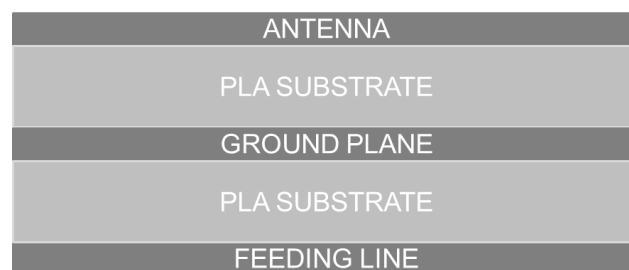


Fig. 1. Stack-up of the layers.

### 2.2. Antenna system design

The overall size of the 3U CubeSat for the antenna design is  $10 \times 10 \text{ cm}^2$  for the bottom face. Indeed, the larger  $30 \times 10 \text{ cm}^2$  sides are generally dedicated to the solar arrays for the energy production. An S-band printed patch antenna has been developed since printed patches seem to be the best candidate for the

communication subsystem [14]. Four rectangular patches with a PLA substrate are proposed to achieve a radiation pattern that can be reconfigured as desired.

An optimization process has been executed with CST MWS, taking into account as starting dimensions those obtained by analytic evaluations. Each rectangular radiator has been firstly optimized in terms of dimensions and location of the feeding point. The dimensions of the rectangular patches are:  $l = 41.75$  mm and  $w = 12$  mm. The position of the patch feeding point has been optimized by EM simulations in order to achieve the best matching, and it is designed 3 mm away from the antenna center (red points in Fig. 2).

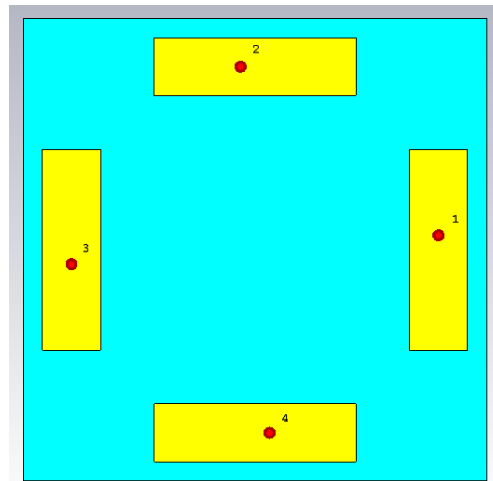


Fig. 2. Antenna system geometry with the 4 feeding points (red circles).

Fig. 3 shows the S-parameter for each patch of the antenna system. In particular, results show the antenna is well matched at the working frequency, since the  $S_{11}$  is lower than -10 dB at 2.45 GHz. In particular, the  $S_{11}$  value is -22.13 at 2.45 GHz.

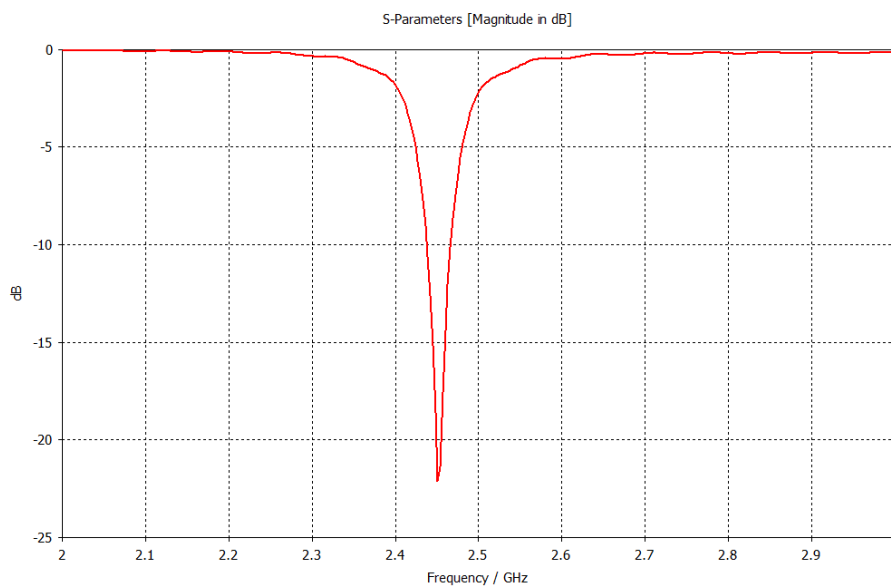


Fig. 3. Return loss of the single patch.

### 2.3. Phase effect on the antenna radiation pattern

MWS CST simulations have been conducted with the four feeding ports, positioned in the four optimized points shown in Fig. 2, changing the phase of the signals in order to analyse antenna radiation pattern, polarization and the gain in relation to the phase at the excitation ports.

Numerous cases have been considered. In the following, three examples are shown.

In the first case, ports 1, 2, 3, and 4 (see Fig. 2) are excited with a phase of  $0^\circ$ ,  $90^\circ$ ,  $180^\circ$ ,  $270^\circ$ , respectively, which means that the two patches are in antiphase between each other and in quadrature with the other two. Regarding the radiation pattern, Fig. 4-1 shows that the maximum radiation is along the boresight with an aperture ( $-3$  dB) of  $57.7^\circ$  and a main lobe directivity of about 8 dBi. Moreover, this configuration exhibits a circular polarization, since the simulated axial ratio values are about equal to 1 and the phase shift  $\cong 90^\circ$  [15].

In the second case, ports 1, 2, 3 and 4 are excited with a phase of  $0^\circ$ ,  $90^\circ$ ,  $180^\circ$ ,  $90^\circ$ , respectively (two opposite patches are in antiphase and the other two in-phase and in quadrature with the other two). The antenna radiation pattern has a heart shape and its maximum at  $30^\circ$  is equal to 6.2 dBi (Fig. 4-2). Moreover, this configuration exhibits a linear polarization.

In the third case, all the ports are excited in phase. Concerning the antenna radiation pattern, the third case shows a polar plot of the simulated with an apple shape with a maximum in the directivity at  $43^\circ$  (Fig. 4-3) and a linear polarization.

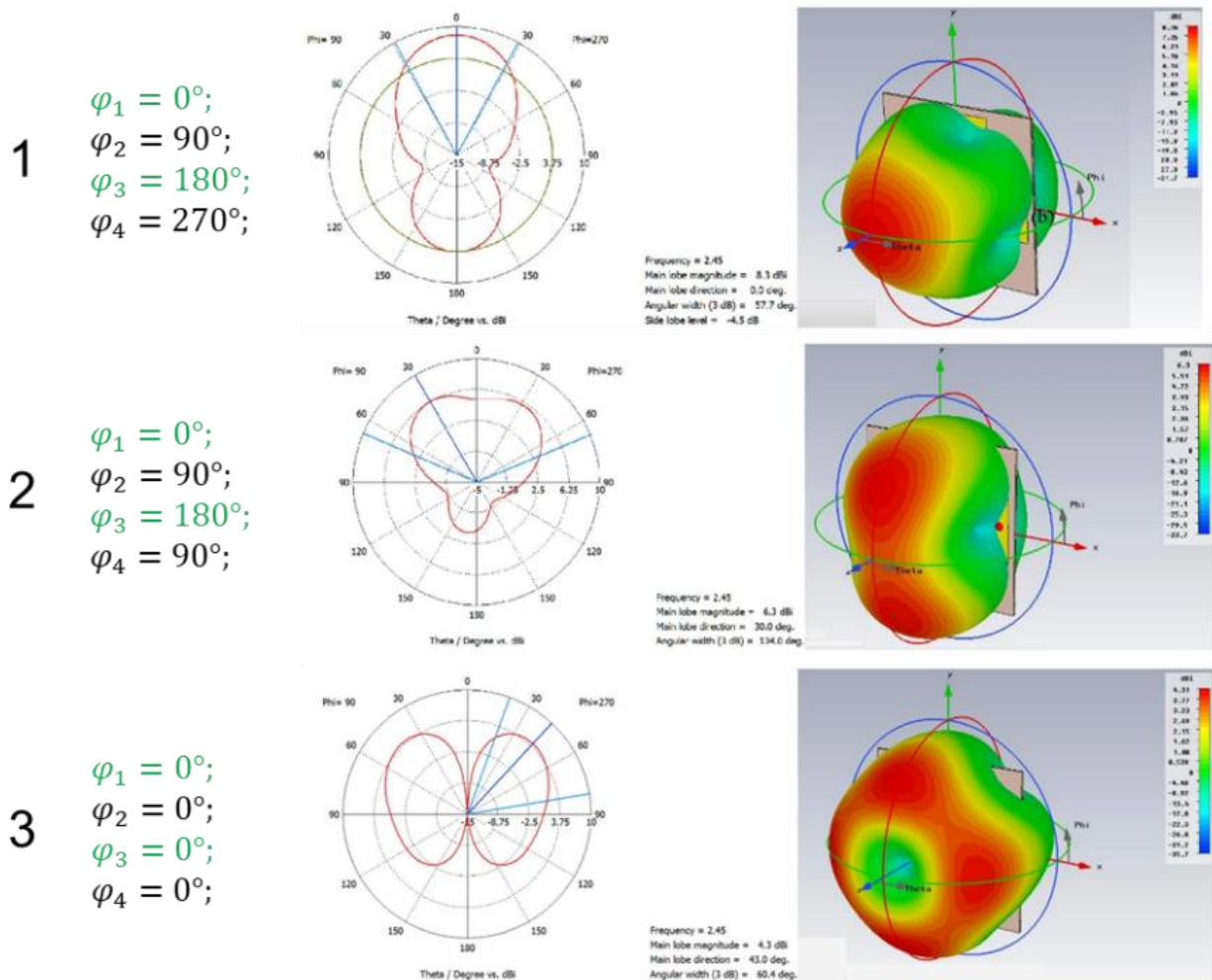


Fig. 4. Feeding signal phase effect on the radiation pattern of the antenna.

#### 2.4. Feeding line design

The feeding line has been designed with MWO. A Wilkinson power divider in microstrip technology is used, with the aim to achieve the chosen radiation pattern. Three power dividers have been used to divide the input power among the four antennas. The feeding line layout is shown in Fig. 5 together with the antenna system in a top view of the layer stack-up. A surface mount phase shifter component can be used as for example the one reported in [16], with a controlled  $0^{\circ}$ - $180^{\circ}$  phase range, or a digital phase shifter [17] to achieve the different input phases. Furthermore, the feeding line, the pad for the SMA connector and the antenna can be built with a conductive filament, such as the Electrifi Conductive Filament by Multi3D [18, 19].

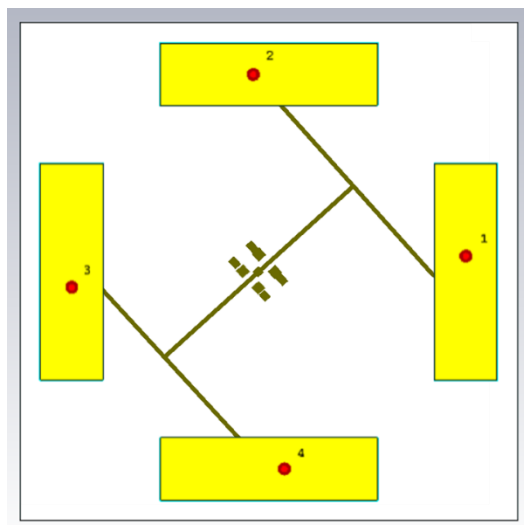


Fig. 5. Antenna system and feeding line top view. At the center of the figure, there are metal pads to solder the SMA connector.

The transmission coefficient is shown in Fig. 6: it has a value around  $-6.1$  dB that entails the power is divided by four, while Fig. 7 shows an about  $0^{\circ}$  phase-shift between the ports.

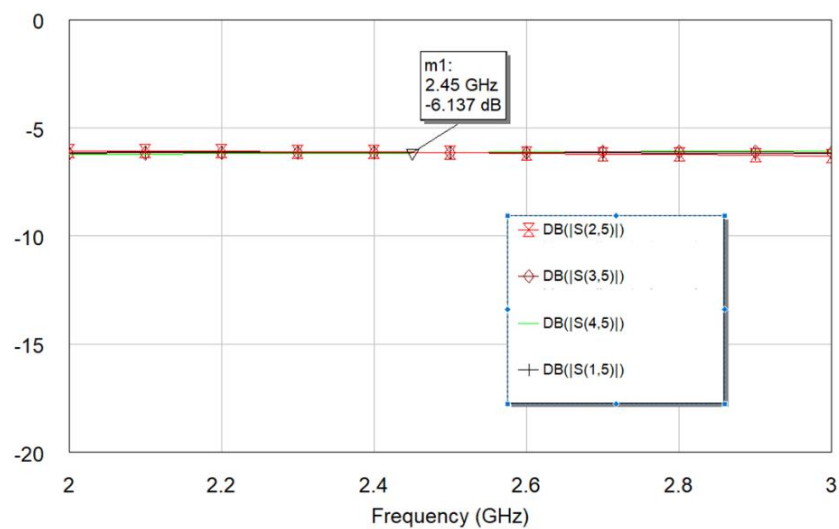


Fig. 6. Transmission coefficient.

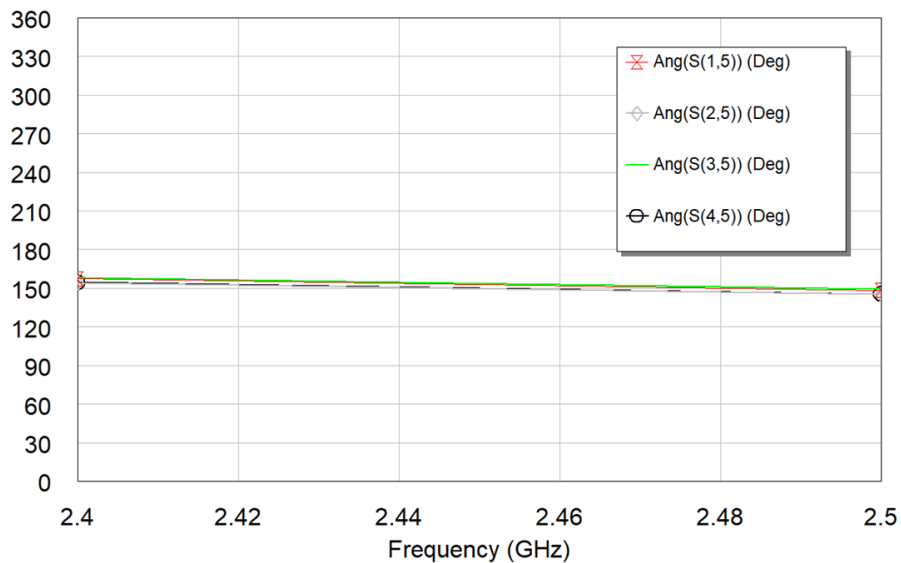


Fig. 7. Shift of the phase between the four ports.

### 3. Results

The entire structure, i.e. the antenna system with the designed feeding line, has been simulated by using CST MWS, including the SMA connector model that will be used in practice to feed the antenna.

#### 3.1. Return loss

Fig. 8 shows the S-parameter of the whole structure computed with MWS: the antenna appears well matched around 2.45 GHz, since at this frequency the return loss is well below the value of -10 dB.

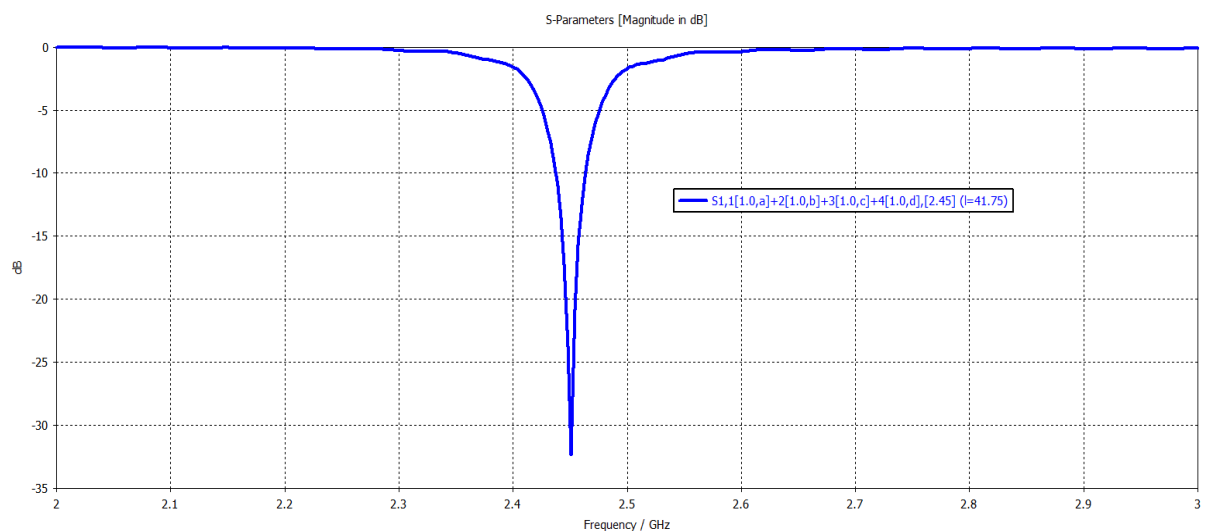


Fig. 8. Simulated return-loss of the complete antenna system (feeding line, patches and SMA connector).

#### 3.2. Radiation pattern

The 3-D radiation pattern plot of the simulated antenna is shown in Fig. 9. The shown case is the 3-D directivity polar plot with an apple shape that has a maximum of about 4 dBi at 45°.

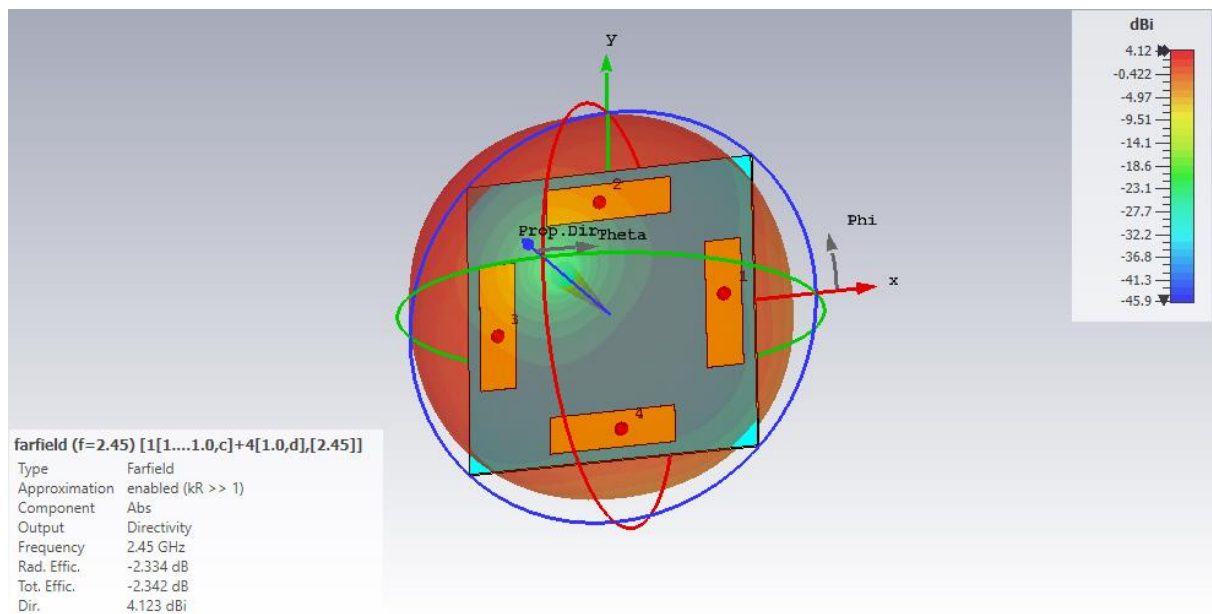


Fig. 9. Simulation results of the 3-D directivity radiation pattern.

#### 4. Conclusion

An S-band patch antenna is proposed, having low cost, compact size and design features appropriate for any CubeSat standard structure. In particular, in order to use the antenna system in space missions with different purpose, feeding line phases have been studied in order to obtain different pattern shapes and field polarizations. The proposed structure has been designed with a numerical EM CAD, simulating a dielectric substrate mimicking the PLA filament (Filofalfa<sup>®</sup>) that was characterized in a previous work. Results point out that the antenna system return loss is lower than -10 dB at the operational frequency. As future developments the antenna system prototype will be manufactured and tested using a 3D printer as for example the Raise3D Pro2 dual extruder printer [20].

#### References

- [1] M. N. Sweeting, "Modern Small Satellites—Changing the Economics of Space," in *Proceedings of the IEEE*, vol. 106, no. 3, pp. 343-361, March 2018.
- [2] "A space science boom or death by a thousand small satellites". *Nat Astron* 4, 1011 (2020). <https://doi.org/10.1038/s41550-020-01257-0>
- [3] H. Hakima, M. C.F. Bazzocchi, M. Reza Emami, "A deorbiter CubeSat for active orbital debris removal", *Advances in Space Research*, vol. 61, no. 9, 2018, pp. 2377-2392.
- [4] M. Maffei, A. Aubry, A. De Maio and A. Farina, "Spaceborne Radar Sensor Architecture for Debris Detection and Tracking," in *IEEE Transactions on Geoscience and Remote Sensing*, vol. 59, no. 8, pp. 6621-6636, Aug. 2021, doi: 10.1109/TGRS.2020.3029384.
- [5] S. Raguraman, R. N. S. Sarath and J. Varghese, "Space Debris Removal: Challenges and Techniques-A Review," 2020 8th International Conference on Reliability, Infocom Technologies and Optimization, 2020, pp. 1361-1366, doi: 10.1109/ICRITO48877.2020.9197877.
- [6] N. P. Khanolkar, N. Shukla, V. Kumar and A. Vats, "Advanced space debris removable technique and proposed laser ablation technique: A review," 2017 International Conference on Infocom Technologies and Unmanned Systems, 2017, pp. 854-858, doi: 10.1109/ICTUS.2017.8286125.
- [7] S. Gao, Y. Rahmat-Samii, R. E. Hodges and X. Yang, "Advanced Antennas for Small Satellites", in *Proceedings of the IEEE*, vol. 106, no. 3, pp. 391-403, March 2018, doi: 10.1109/JPROC.2018.2804664.



- [8] Panel on Frequency Allocations Spectrum Protection for Scientific Uses, Committee on Radio Frequencies, National Research Council, Handbook of Frequency Allocations and Spectrum Protection for Scientific Uses. The National Academies Press, 2007.
- [9] E. Pittella et al., “Reconfigurable S-band patch antenna system for cubesat satellites,” in IEEE Aerospace and Electronic Systems Magazine, vol. 31, no. 5, pp. 6-13, May 2016.
- [10] Tomaszewska, et al., “Products of sugar beet processing as raw materials for chemicals and biodegradable polymers”, RSC Advances, 2018,8, 3161-3177.
- [11] <https://www.filoalfa3d.com/it/>
- [12] E. Pittella, L. D'Alvia, E. Palermo and E. Piuze, “Microwave Characterization of 3D Printed PLA and PLA/CNT Composites”, 6<sup>th</sup> online Forum on Research and Technologies for Society and Industry, Innovation for a smart world, September 6-9, 2021.
- [13] Smiths, “PTFE (Polytetrafluoroethylene) Technical Datasheet.
- [14] E. Pittella et al, “Reconfigurable S-Band Patch Antenna Radiation Patterns for Satellite Missions,” 2018 5<sup>th</sup> IEEE International Workshop on Metrology for AeroSpace, 2018, pp. 651-656.
- [15] C. A. Balanis, Antenna Theory Analysis and Design, Fourth Edition, Wiley, 2016.
- [16] Surface Mount Phase Shifter JSPHS-2484+, <https://www.minicircuits.com/pdfs/JSPHS-2484+.pdf>
- [17] Analog Device, HMC647a, Gaas MMIC 6-BIT Digital Phase Shifter, 2.5-3.1 GHz.
- [18] <https://www.multi3dllc.com/>
- [19] Y. Xie, S. Ye, C. Reyes, P. Sithikong, B.-I. Popa, B. J. Wiley, S.A. Cummer, “Microwave Metamaterials Made by Fused Deposition 3D Printing of a Highly Conductive Copper-Based Filament”, Appl. Phys. Lett. vol. 110, no. 18, April 2017.
- [20] <https://www.raise3d.com/pro2/>